

Computational Fluid Dynamics Modeling of Proton Exchange Membrane Fuel Cells using Fluent[®]

Ugur Pasaogullari, Chao-Yang Wang[†]
*Electrochemical Engine Center
The Pennsylvania State University
University Park, PA, 16802*

A comprehensive multi-physics model has been developed to simulate proton exchange membrane fuel cells using commercially available CFD software Fluent[®]. The developed model accounts simultaneously for electrochemical kinetics and multi-component species transport. The proposed model is a full cell model, which includes all the parts of the PEM fuel cell, flow channels, gas diffusion electrodes, catalyst layers and the membrane. Coupled transport and electrochemical kinetics equations are solved in a single domain; therefore no interfacial boundary condition is required at the internal boundaries between cell components. The model incorporates the various modes of water transport; therefore it is able to provide comprehensive water management study, which is essential for PEM fuel cells in order to achieve high performance. The model is capable of simulating the fuel cell under a variety of reformat fuel for real life applications. The model is tested against available experimental data and previously published models. Since the model has been developed using the commercial software Fluent[®], it can be easily applied for different flow field designs. Finally, the model is applied to several different operating conditions with different cell geometries and corresponding results are reported, including the effect of different flow fields on cell performance. **Keywords:** PEM, Fuel Cell, Mathematical Modeling, Water Management, Interdigitated Flow Field, Nafion[®]

[†] Corresponding Author cxw31@psu.edu

Nomenclature

A	Superficial Electrode Area, m^2
C	Molar Concentration, mol/m^3
D	Species Diffusivity, m^2/s
I	Current Density, A/m^2
S	Source Terms in Transport and Phase Potential Equations
U	Inlet Velocity, m/s
j	Transfer Current Density, A/m^3
\vec{u}	velocity vector, m/s
p	<i>pressure, Pa</i>

Greek Letters

η	Overpotential, V
ρ	density, kg/m^3
ε	porosity
σ	Ionic Conductivity, S/m
Φ	Phase Potential, V
ζ	Stoichiometric Coefficient
ϑ	Volumetric Flow Rate, m^3/s
λ	Water Content of The Membrane
μ	Viscosity, $kg\ m/s$

Introduction

In recent years, the interest in development of fuel cell systems has accelerated. Higher energy density and less polluting energy conversion promise of these devices make them feasible for use in stationary, portable and automotive applications. In particular, for automotive and portable applications, the Proton Exchange Membrane Fuel Cells are considered as the most successful candidates for replacing current power generating devices. Their high energy efficiency potential, possibly up to 50-70 %, which is unlimited to Carnot cycle efficiency, very low greenhouse emissions, quieter and reliable operation because of none or limited number of moving parts and scalability allow them to replace Internal Combustion Engines for vehicle applications and batteries for portable devices.

Like any electrochemical device, A Proton Exchange Membrane (PEM) Fuel Cell system consists of an anode, a cathode and an electrolyte. A polymer membrane is used as the electrolyte in PEM Fuel Cell systems. Each one of the anode and cathode electrodes consist of gas channel, gas diffuser and catalyst layer, in which the electrochemical reactions take place. A Proton Exchange Membrane fuel cell is illustrated in Figure 1.

The performance of the fuel cell system is characterized by current-voltage curve (*i.e. polarization curve*). The difference between the open circuit potential of the electrochemical reaction and cell voltage occurs from the losses associated with the operation. The corresponding voltage drop is generally classified in three parts:

- i. activation over-potential caused by the electrochemical reactions,
- ii. ohmic drop across the polymer electrolyte

iii. mass transfer limitations of reactants

These associated losses dominate over different current density ranges. For low current densities; the activation over-potential is dominant. For high current densities, which are of particular interest for vehicle applications because of higher power density; the mass transfer limitations dominates the losses. For moderate current densities, the ohmic drop across the polymer membrane dominates. Moreover, for high current densities, water starts to exist in liquid form leading to a two-phase transport of reactants to reaction site, which is an additional transport phenomenon of PEM Fuel Cell operation.

For optimal design and operation of PEM fuel cell system, a careful and detailed understanding of transport and electrochemical kinetics is necessary. Several studies accounting for this purpose has been published over the decades. The PEM fuel cell research up to mid 1990's is exclusively reviewed by Prater [1] and Gottesfeld [2] in different studies. Moreover, in recent years, different numerical models of PEM Fuel Cells are also published by different groups. Early models by Bernardi and Verbrugge [3] and Springer *et al.* [4] are essentially one-dimensional models. Fuller and Newman [5], Nguyen and White [6], Gurau *et al.* [7] and Yi and Nguyen [8] presented pseudo-two dimensional models, which account for variations in compositions along the flow path. Recently, Um *et al.* [9] has published a multi-dimensional CFD model of PEM Fuel Cells based on the approach developed for battery systems by Gu *et al.* [10]

The objective of this study is to extend the applicability of the model by Um *et al.* by considering the additional physics involved in the water transport. Water management is highly critical in PEM Fuel Cell applications. In order to achieve high performance, the

ohmic losses should be minimized, therefore, the membrane should be hydrated, on the other hand at the high current densities the water produced in the cathode catalyst layer starts to condense at the cathode side, therefore hindering the oxygen transport and lowering the performance. A detailed analysis of water transport, involving different modes of transport is added to the previous model of Um et al. The proposed model is solved using commercially available CFD software Fluent[®], using User Defined Functions to customize the solver to meet the purpose. The other goal of this study is to investigate the effects of different flow field designs on the PEM Fuel Cell performance.

In the following sections, development of a Fluent[®] based multi-dimensional, multi-physics PEM Fuel Cell model is described. The validation of model against available experimental data is also provided.

Model Development

It is previously noted that the proposed model is based on the model of Um *et al.* and suited particularly for commercially available CFD software Fluent[®]. The model developed by Um *et al.* based on the battery systems modeling by Gu *et al.* and it is formulated for single domain. Therefore, unlike the model presented by Gurau *et al.*, the proposed model does not require any internal boundary conditions between the components of PEM Fuel Cell system.

A PEM Fuel Cell system consists of gas channels, gas diffusers, catalyst layers and a polymer membrane, as shown in Figure 1. The different physical properties and transport parameters are incorporated into a single set of governing equations using a single domain formulation. The model aims to study the electrochemical kinetics, current distribution, reactant flow fields and multi-component transport of oxidizer and fuel streams in a multi-dimensional domain. The assumptions made in developing the model are as follows:

- Ideal gas mixtures
- Incompressible and Laminar flow because low flow velocities and low fuel utilization
- Isotropic and homogeneous porous electrodes, catalyst layers and membrane
- Isothermal operation
- Negligible ohmic resistance at porous electrodes and current collectors

Under isothermal conditions, fuel cell operation is governed by the mass, momentum, species and charge conservation equations. The conservation equations of mass, momentum, species and charge that are suited for Fluent[®], is as follows:

$$\frac{\partial(\rho\varepsilon)}{\partial t} + \nabla \cdot (\varepsilon\rho\vec{u}) = 0 \quad (1)$$

$$\frac{\partial(\rho\varepsilon\vec{u})}{\partial t} + \nabla \cdot (\varepsilon\rho\vec{u}\vec{u}) = -\varepsilon\nabla p + \nabla \cdot (\varepsilon\mu\nabla\vec{u}) + S_u \quad (2)$$

$$\frac{\partial(\varepsilon C_k)}{\partial t} + \nabla \cdot (\varepsilon\vec{u}C_k) = \nabla \cdot (D_k^{eff}\nabla C_k) + S_k \quad (3)$$

$$\nabla \cdot (\sigma_g^{eff}\nabla\Phi_e) + S_\Phi = 0 \quad (4)$$

, where \vec{u}, C_k, Φ_e denotes intrinsic velocity vector, molar concentration of k^{th} species and electrolyte phase potential, respectively.

The corresponding source terms treating the electrochemical reactions and porous media are presented in Table 3.

It is of benefit to further explain the corresponding diffusivities of the governing equations. The diffusivities for species concentration equations and ionic conductivity for membrane phase potential equation are modified using Bruggeman correlation to account for porous electrodes, which can be expressed as:

$$D_k^{eff} = \varepsilon_m^{1.5} D_k \quad (5)$$

$$\sigma_e^{eff} = \varepsilon_m^{1.5} \sigma_e \quad (6)$$

In a fuel cell system, the inlet flow rates are generally expressed as stoichiometric ratios of inlet streams based on a reference current density. The stoichiometric ratios inlet streams are given by the following equations.

$$\zeta^{anode} = C_{H_2} \vartheta^{anode} \frac{2F}{I_{ref} A} \quad (7)$$

$$\zeta^{cathode} = C_{O_2} \vartheta^{cathode} \frac{4F}{I_{ref} A} \quad (8)$$

The local current density is calculated as:

$$I(y, z) = \sigma_e^{eff} \frac{\partial \Phi_e}{\partial x} \quad (9)$$

And the average current density is:

$$I_{avg} = \frac{1}{A} \iint_A I(y, z) dydz \quad (10)$$

More details of developed model is presented in the previous study published by Um *et al.* [9]

In a fuel cell system, water management has a significant impact on performance. Besides, water vapor has more complex transport mechanism than any other species present in PEM fuel cell operation. In the following section, treatment of water transport in proposed model is explained.

Water Transport

In PEM Fuel Cells, due to properties of Polymer Electrolyte Membrane, the water molecules are transported via electro-osmotic drag in addition to the molecular diffusion. Water molecules are transported through the polymer electrolyte membrane by the H⁺ protons, and this transport phenomenon is called electro-osmotic drag. In addition to the molecular diffusion and electro-osmotic drag, water vapor is also produced in the cathode catalyst layer due to Oxygen Reduction Reaction. The transport of water has been illustrated in Figure 2.

Water transport through the polymer electrolyte membrane has been investigated by several researchers in different aspects. Most interesting studies in this area includes the determination of water diffusion coefficient [11] and water drag coefficient [12] by

Zawodzinski *et al.* and investigating the diffusion of water in Nafion[®] membranes by Motupally *et al.*[13]

The electro-osmotic drag coefficient is defined as the number of water molecules transported by each hydrogen proton H⁺. The electro-osmotic drag coefficient can be expressed with the following equation:

$$n_d = \frac{2.5\lambda}{22} \quad [4] \quad (11)$$

The diffusion coefficient of water in Polymer Membrane is also highly dependent on the water content of the membrane. The relation is given as:

$$D_W^m = \left\{ \begin{array}{l} 3.1 \cdot 10^{-7} \cdot \lambda \cdot (e^{0.28\lambda} - 1) \cdot e^{-2346/T} \text{ for } 0 < \lambda < 3 \\ 4.17 \cdot 10^{-8} \cdot \lambda \cdot (1 + 161 \cdot e^{-\lambda}) \cdot e^{-2346/T} \text{ otherwise} \end{array} \right\} \quad [13] \quad (12)$$

Boundary Conditions

The previously noted set of equations, which governs the fuel cell operation forms (m+5) unknowns, where m is the physical dimension of the problem domain. There are natural boundary conditions of zero-flux prescribed everywhere other than the inlet and outlets of the flow channels. The boundary conditions prescribed at the inlets of the gas channels are:

$$\begin{aligned} U_{in}^{anode} &= U_a^0, U_{in}^{cathode} = U_c^0 \\ C_{H_2}^{anode,in} &= C_{H_2}^0, C_{O_2}^{cathode,in} = C_{O_2}^0 \\ C_{H_2O}^{anode,in} &= C_{H_2O}^{0,a}, C_{H_2O}^{cathode,in} = C_{H_2O}^{0,c} \end{aligned} \quad (11)$$

Numerical Procedure

The governing equations, (1) through (4) are solved using the commercially available CFD software Fluent[®]. The software is customized using User Defined

Functions to be able solve the electrochemical kinetics, since the software is not capable of modeling electrochemical systems. A mesh of 130x100x62 was found to provide required spatial resolution for five-channel geometry. The solution is considered to be converged when the difference between successive iterations is less than 10^{-7} for all variables. The computation time for the geometry described above is around 7 hours on a 1.7 GHz PC.

Results & Discussion

The experimental data of Ticianelli *et al.* [14] is used to validate the results obtained from numerical simulations. In Figure 3, the computed polarization curve is compared the experimental results of Ticianelli *et al.* and it is seen that the calculated results are in good agreement with the experimental data.

Unlike the published experimental results, the proposed model is capable of providing more detailed data regarding the operation of fuel cell system, including the flow field, species concentration and current density distribution.

To illustrate the capability of the proposed model and to investigate the effect of flow field design on fuel cell performance, three different test cells are simulated. The dimensions of these test cells are given in Table 3. The different flow fields used in these three test cells are illustrated in Figure 4.

The Electrochemical and Transport Parameters used in these simulations are summarized in Table 1, and the operational parameters are presented in Table 2.

In Figure 5, the current density distributions at a cell voltage of 0.4 V for three different designs are provided. The average current densities are calculated as: 0.965 A/cm² for straight anode channel and straight cathode channel design, 1.035 A/cm² for serpentine anode channel and serpentine cathode channel design and 1.356 A/cm² for serpentine anode channel and interdigitated cathode channel design.

It is seen that there is almost 30% increase in the cell performance, when an interdigitated flow pattern is used in the cathode side. With the interdigitated flow pattern, the flow is forced through the porous gas diffusers, therefore accelerating the

transport of reactants to the reaction site, resulting in increase of performance. This forced convection also carries away more water produced in the catalyst layer, which is produced as a result of the oxygen reduction reaction.

When the results are further investigated, it is seen that the current density distribution is more uniform in third design than the other two. In the serpentine or straight designs, a significant difference is noticed in the regions underneath of the current collector and the gas channel.

Figure 6 displays the species molar concentrations for three different designs. It is seen that for all designs at this cell voltage, the water vapor molar concentration exceeds the saturated value, which means that condensation takes place. Therefore, this model can be just illustrative at these cell voltages, a more-realistic multi-phase model is necessary to fully simulate these current densities. Moreover, it is noted that at the inlet of gas channels, there is net water vapor transport from anode to cathode due to electro-osmotic drag. Then, the electro-osmotic drag is balanced by molecular diffusion from cathode to anode, since water vapor concentration is higher in cathode due to Oxygen Reduction Reaction.

Figure 7 shows calculated current density distribution along the channel to channel direction. This figure illustrates the difference in the current density between the regions underneath the current collector and the flow channel. In the regions underneath the current collector, the convective transport is limited compared to the region underneath the flow channel, therefore the electrochemical reaction is hindered, resulting in lower current density. However, this effect is not seen in interdigitated flow field

design, since the flow is forced into the porous media, therefore increasing the convective transport under the current collectors.

It is seen that fuel cell performance is highly improved by using interdigitated flow pattern in the mass transfer limited zone of polarization curve. Interdigitated flow fields are also effective in removing the excess water by providing additional convective transport in the gas diffuser.

Conclusions

A three dimensional model has been developed and applied to three different designs in order to investigate the effects of flow field on to PEM Fuel Cell Performance. The effect is illustrated through the two-dimensional contours of current density for different designs and three dimensional plots of species concentrations. The developed model, which incorporated the electrochemical kinetics and multi-dimensional species transport can be used to understand the complex electrochemistry occurring during the fuel cell operation and simulating the actual operating conditions as a tool for design of PEM Fuel Cells.

References

- [1] K. B. Prater, *J. Power Sources*, **51**, 129 (1994)
- [2] S. Gottesfeld, in *Advances in Electrochemical Science and Engineering*, C. Tobias, Editor, Vol. 5, p.195, *John Wiley and Sons, New York* (1997)
- [3] D. M. Bernardi and M. W. Verbrugge, *J. Electrochem. Soc.*, **139**, 2477 (1992)
- [4] T. E. Springer, M. S. Wilson and S. Gottesfeld, *J. Electrochem. Soc.*, **140**, 3513 (1993)
- [5] T. F. Fuller and J. Newman, *J. Electrochem. Soc.*, **140**, 1218 (1993)
- [6] T. V. Nguyen and R. E. White, *J. Electrochem. Soc.*, **140**, 2178 (1993)
- [7] V. Gurau, H. Liu and S. Kakac, *AIChE J.*, **44**, 2410 (1998)
- [8] J. S. Yi and T. V. Nguyen, *J. Electrochem. Soc.*, **146**, 38 (1999)
- [9] S. Um, C.-Y. Wang and K. S. Chen, *J. Electrochem. Soc.*, **147**, 12 (2000)
- [10] W. B. Gu, C.-Y. Wang, and B. Y. Liaw, *J. Electrochem. Soc.*, **144**, 2053 (1997)
- [11] T. A. Zawodzinski, Jr, M. Neeman, L. O. Sillerud and S. Gottesfeld, *J. Phys. Chem.*, **95**, p.6040, (1991)
- [12] T. A. Zawodzinski, J. Davey, J. Valerio and S. Gottesfeld, *Electrochimica Acta*, **40**, 3 (1995)
- [13] S. Motupally, A. J. Becker and J. W. Weidner, *J. Electrochem. Soc.*, **147**, 9 (2000)
- [14] E. A. Ticianelli, C. R. Derouin and S. Srinivasan, *J. Electroanal. Chem.*, **251**, 275 (1998)

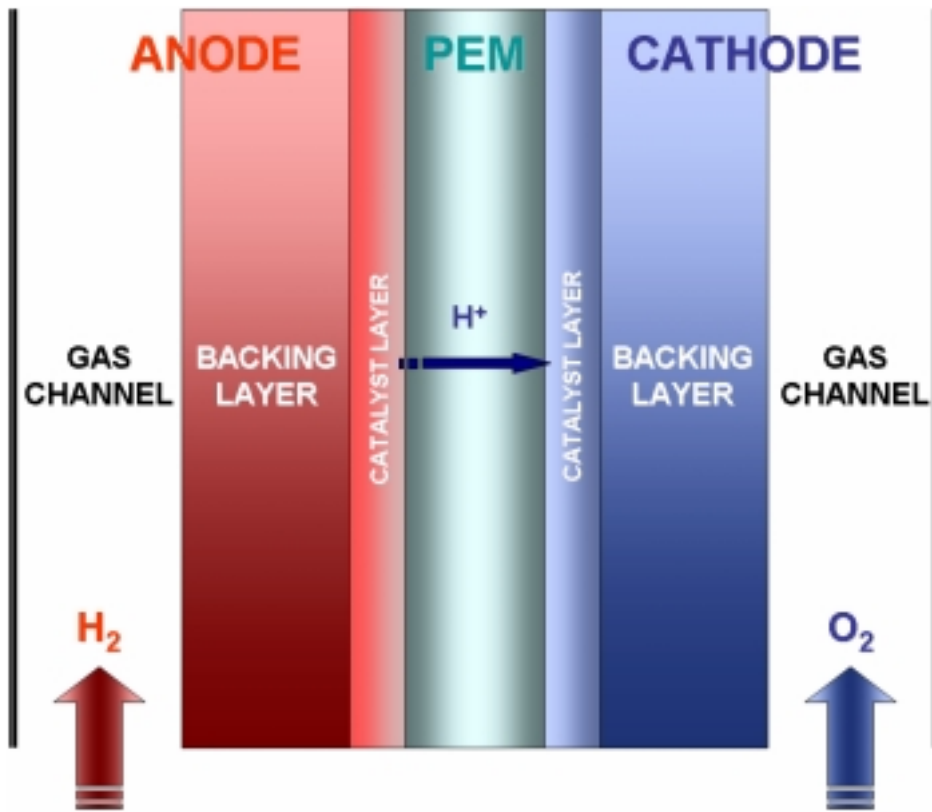


Figure 1 PEM Fuel Cell Schematics

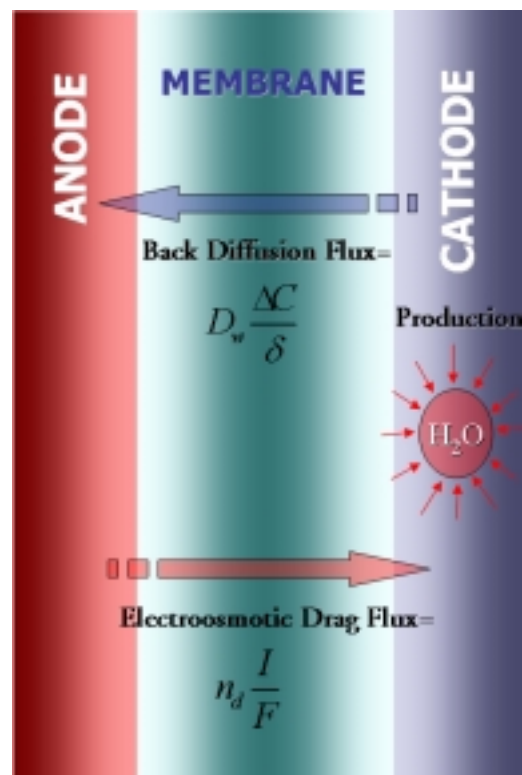


Figure 2 Water Transport in PEM Fuel Cell

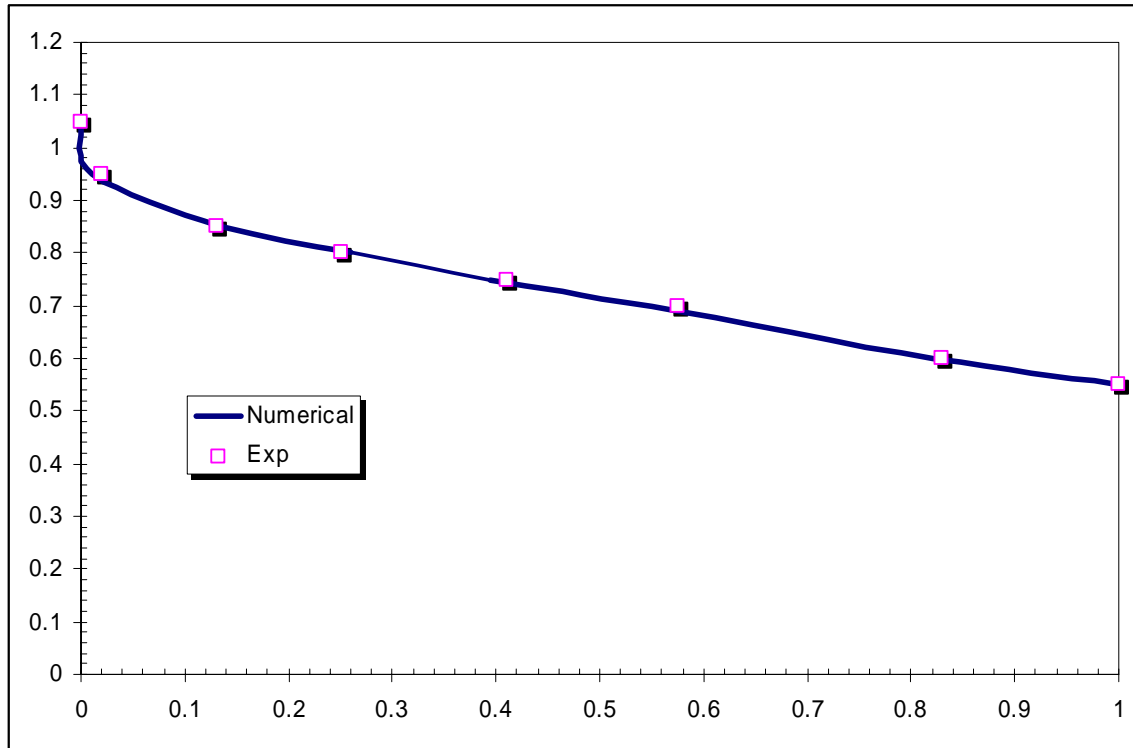


Figure 3 Comparison of Calculated and Measured Polarization Curves
The experimental data is adapted from Ticianelli *et al.* [14]

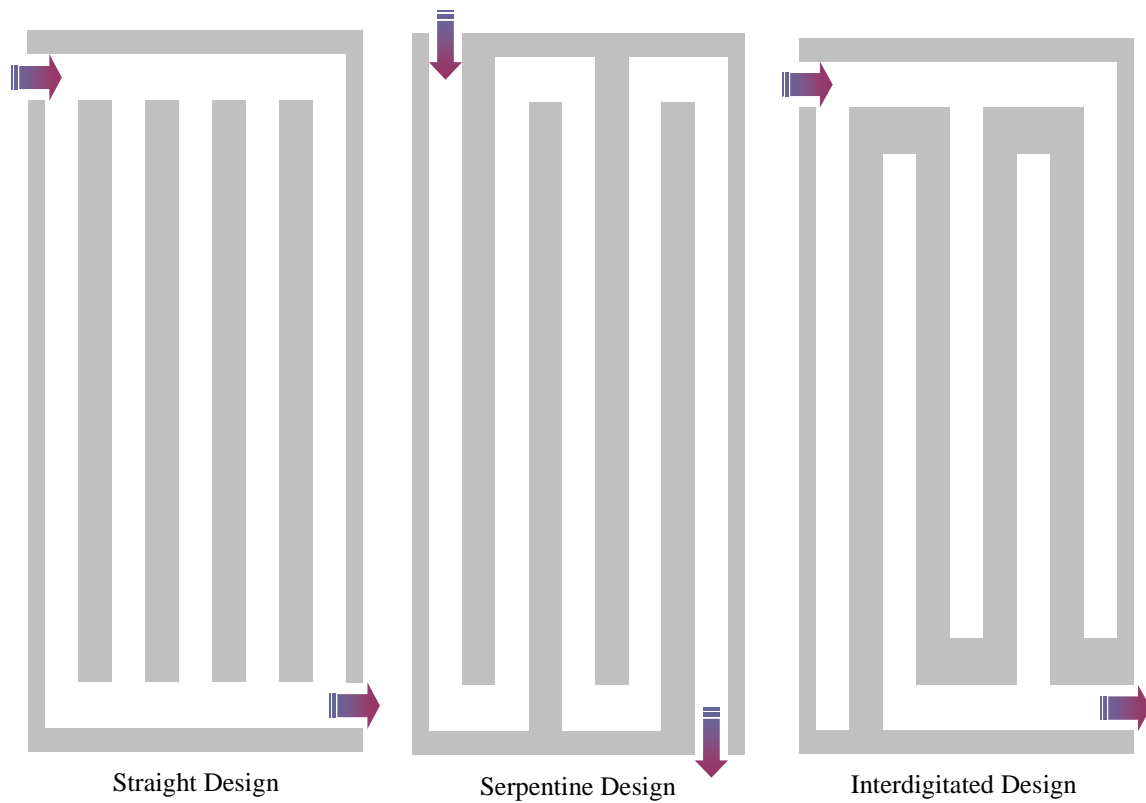


Figure 4 Illustrations of different flow field designs

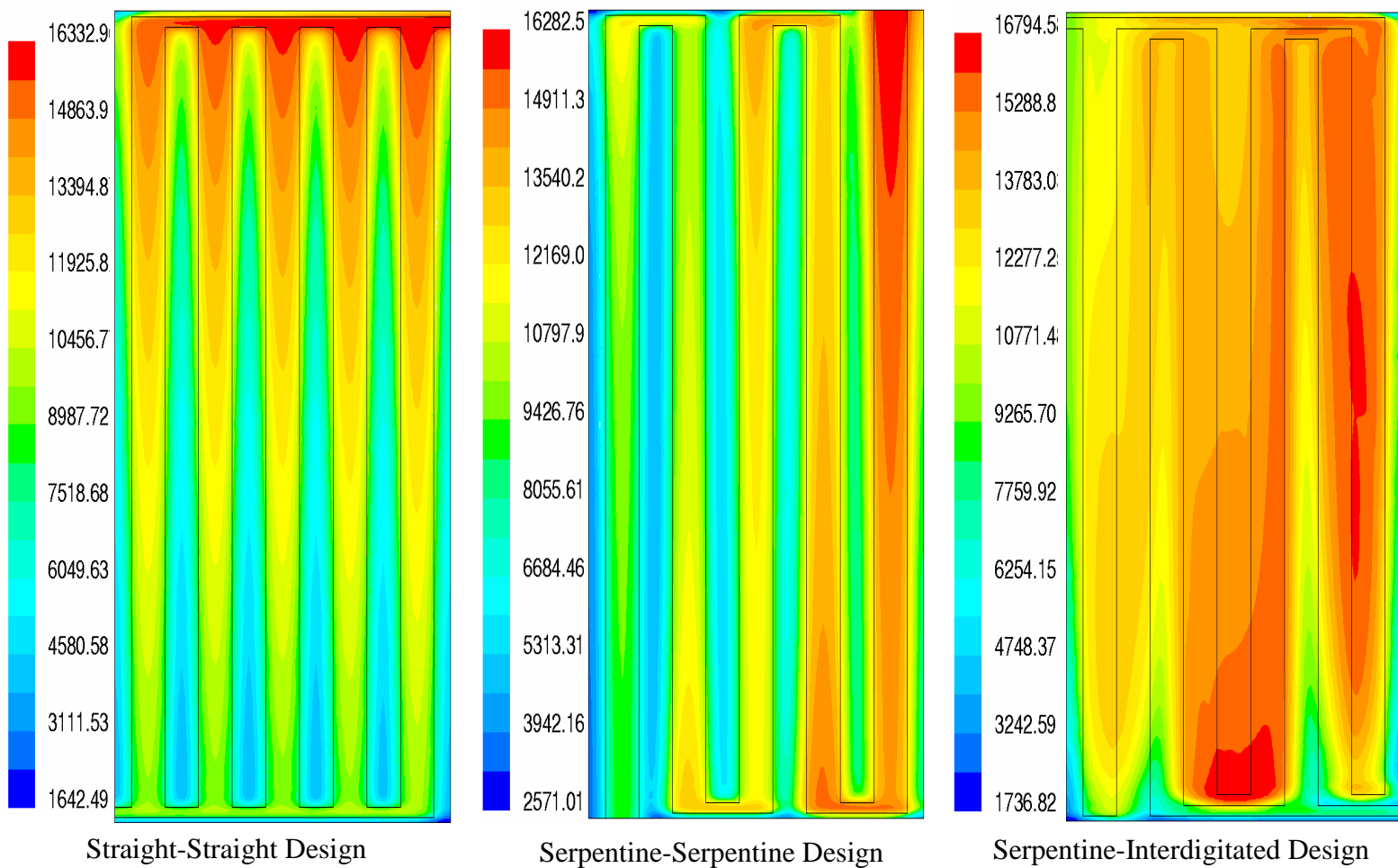


Figure 5 Current Density Distribution for three different designs [A/m^2]
 Fully Humidified Anode and Cathode Inlets, $V_{cell}=0.4$ V and $T_{cell}=353$ K

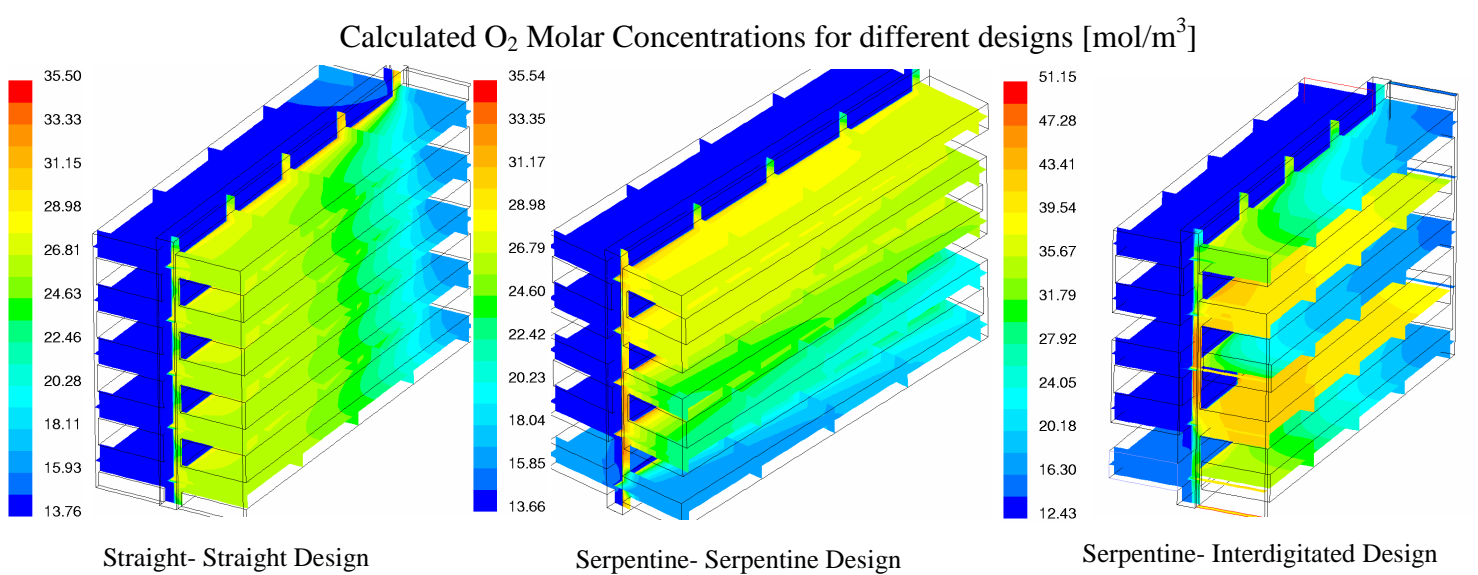
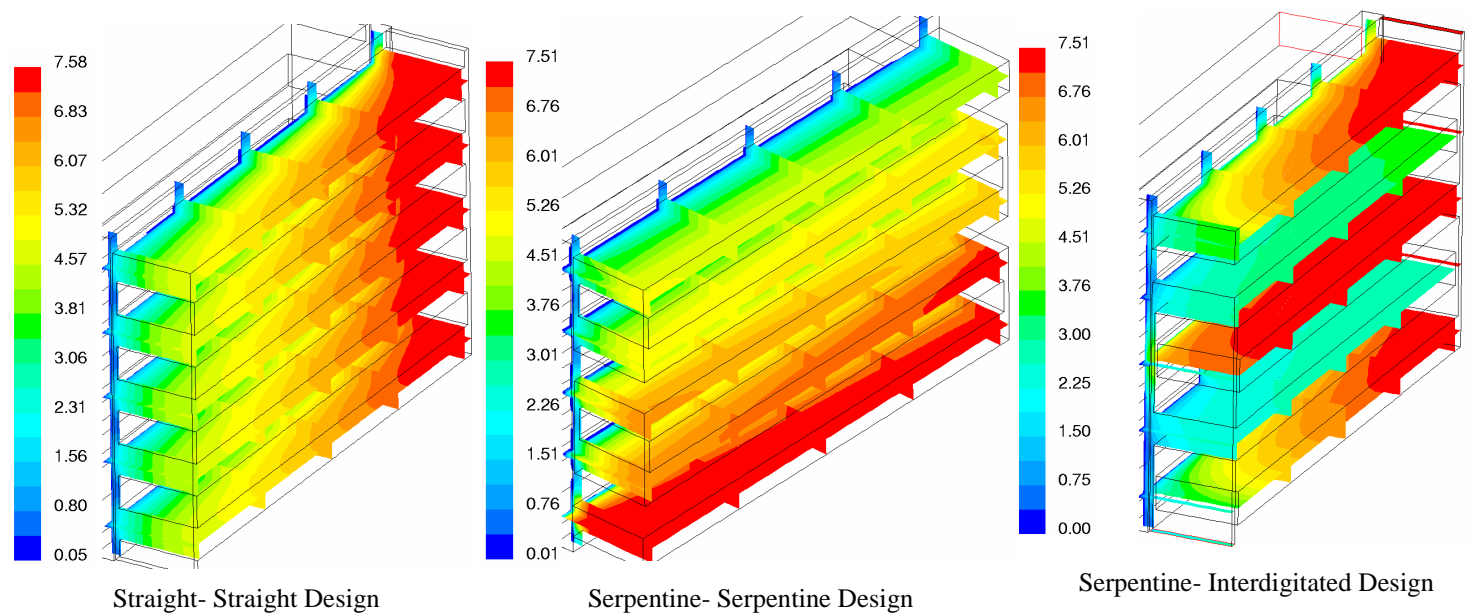
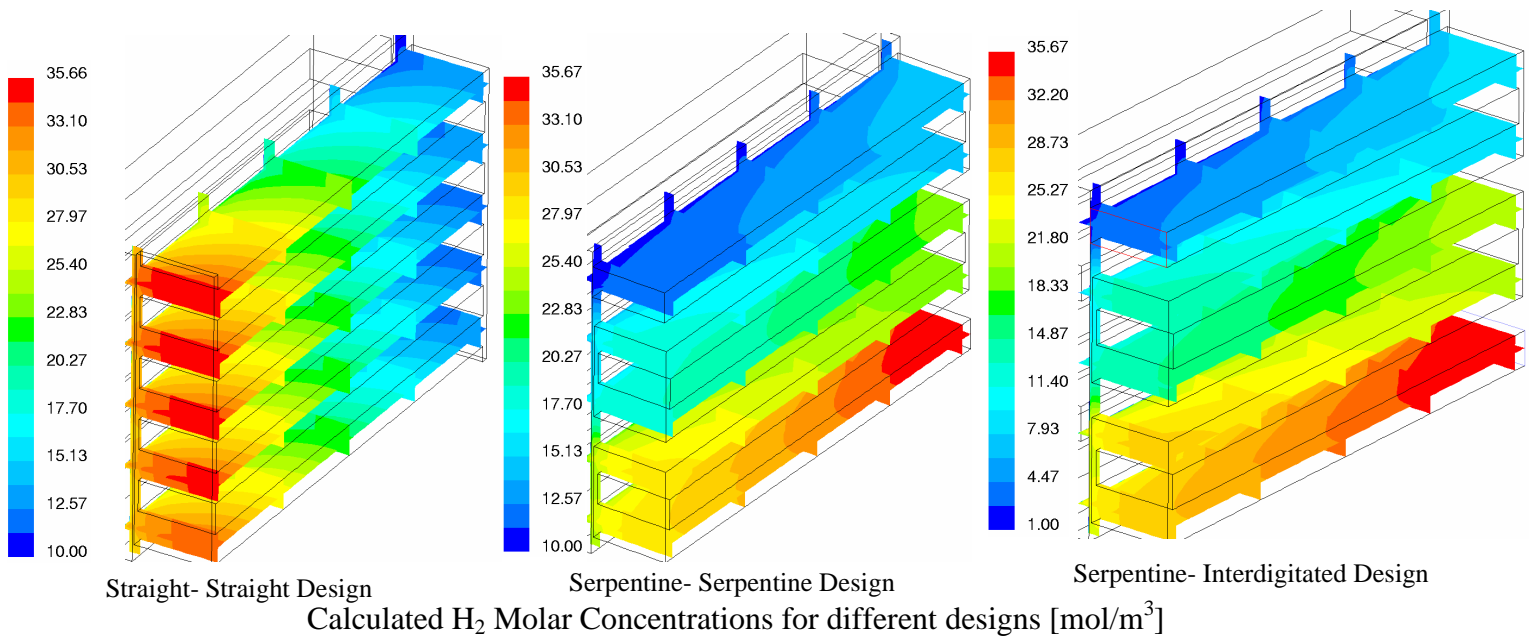


Figure 6 Calculated Species Molar Con centrations for different designs
 Fully Humidified Anode and Cathode Inlets, $V_{\text{cell}}=0.4$ V and $T_{\text{cell}}=353$ K

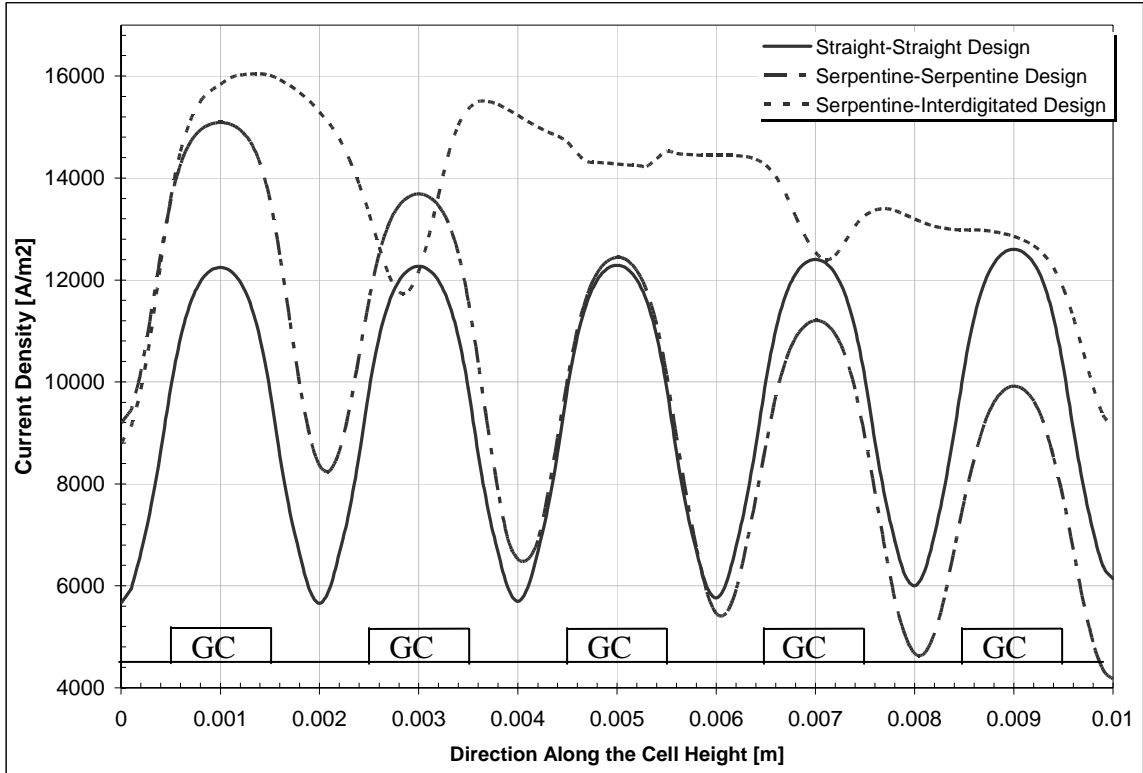


Figure 7 Calculated Current Density Distribution Along the Channel-Channel Direction

$y=L/2$, $V_{\text{cell}}=0.4 \text{ V}$, $T_{\text{cell}}=353 \text{ K}$
GC: Gas Channel

Table 1 Electrochemical and Transport Properties

<i>DESCRIPTION</i>	<i>UNIT</i>	<i>VALUE</i>
Anode reference exchange current density	A/m ³	1.0e9
Anode reference exchange current density	A/m ³	20000.
Anode Transfer Coefficient		2
Cathode Transfer Coefficient		1
Faraday Constant	C/mol	96487.0
H ₂ Diffusivity	m ² /s	7.33e-5
O ₂ Diffusivity	m ² /s	2.13e-5
H ₂ O Diffusivity at Anode	m ² /s	7.33e-5
H ₂ O Diffusivity at Cathode	m ² /s	4.90e-5
Anode Viscosity	m ² /s	2.89e-5
Cathode Viscosity	m ² /s	1.36e-5
Membrane Viscosity	m ² /s	3.56e-4
Material Properties		
Anode Backing Layer Porosity		0.5
Cathode Backing Layer Porosity		0.5
Permeability of Anode Backing Layer	m ²	1.76e-11
Permeability of Cathode Backing Layer	m ²	1.76e-11
Membrane Porosity		0.28
Volume Fraction Of Membrane In Catalyst Layer		0.2
Nafion [®] content in membrane		0.67
Hydraulic Permeability of Membrane	m ²	1.8e-18
Equivalent Weight of Membrane [Nafion [®] 112]	kg/mol	1.1
Dry Density of Membrane [Nafion [®] 112]	kg/m ³	1.98e3

Table 2 Operational Parameters

<i>DESCRIPTION</i>	<i>UNIT</i>	<i>VALUE</i>
Reference Average Current Density	A/cm ²	1.0
Anode Stoichiometric Coefficient based on 1.0 A/cm ²		1.5
Cathode Stoichiometric Coefficient based on 1.0 A/cm ²		2.0
Anode Inlet Pressure	Atm	1.5
Cathode Inlet Pressure	Atm	1.5
Cell Temperature	°C	80
Inlet Molar Concentrations		
<i>Anode: Fully Humidified at 80°C</i>		
Hydrogen	mol/m ³	35.667
Oxygen	mol/m ³	0
Water Vapor	mol/m ³	16.121
<i>Cathode: Fully Humidified at 80°C</i>		
Hydrogen	mol/m ³	0
Oxygen	mol/m ³	7.51
Water Vapor	mol/m ³	16.121

Table 3 Test Cell Dimensions

<i>DESCRIPTION</i>	<i>UNIT</i>	<i>VALUE</i>
Cell Length	mm	76.3
Cell Height	mm	10.0
Current Collector Height	mm	1.0
Gas Channel Height	mm	1.0
Anode Gas Channel Width	mm	2.54
Cathode Gas Channel Width	mm	2.54
Anode Backing Layer Thickness	mm	0.3
Cathode Backing Layer Thickness	mm	0.3
Anode Catalyst Layer Thickness	μm	10
Cathode Catalyst Layer Thickness	μm	10
Membrane Width [Nafion [®] 112]	μm	51
Total Cell Thickness	mm	5.751

Table 4 Source Terms

	S_U (MOMENTUM)	S_K (SPECIES)	S_Φ (PHASE POTENTIAL)
GAS CHANNELS	0		N/A
BACKING LAYERS	$-\frac{\mu}{K} \varepsilon^2 \bar{u}$		
CATALYST LAYERS	$-\frac{\mu}{K} \varepsilon^2 \bar{u}$	$-\frac{j_a}{2F} \frac{\rho}{\varepsilon_m \varepsilon_{mc}}$: anode $\frac{j_c}{4F} \frac{\rho}{\varepsilon_m \varepsilon_{mc}}$: cathode $-\frac{j_c}{F} \left(\frac{1}{2} + n_d\right) \frac{\rho}{\varepsilon_m \varepsilon_{mc}}$: cathode $-\frac{n_d}{F} j_a \frac{\rho}{\varepsilon_m \varepsilon_{mc}}$: anode	H_2 O_2 j H_2O
MEMBRANE	$-\frac{\mu}{K} \varepsilon^2 \bar{u}$		